

# BACK-CONTACTED AND SMALL FORM FACTOR GaAs SOLAR CELL

Cruz-Campa, J. L.<sup>1</sup>; Nielson, G. N.<sup>1</sup>; Okandan, M.<sup>1</sup>; Wanlass, M. W.<sup>2</sup>; Sanchez, C. A.<sup>1</sup>;

Resnick, P. J.<sup>1</sup>; Clews, P. J.<sup>1</sup>; Pluym, T.<sup>1</sup>; Gupta, V. P.<sup>1</sup>

<sup>1</sup> Sandia National Laboratories, Albuquerque, NM, USA

<sup>2</sup> National Renewable Energy Laboratory, Golden, CO, USA

## ABSTRACT

We present a newly developed microsystem enabled, back-contacted, shade-free GaAs solar cell. Using microsystem tools, we created sturdy 3  $\mu\text{m}$  thick devices with lateral dimensions of 250  $\mu\text{m}$ , 500  $\mu\text{m}$ , 1 mm, and 2 mm. The fabrication procedure and the results of characterization tests are discussed below. The highest efficiency cell had a lateral size of 500  $\mu\text{m}$  and a conversion efficiency of 10%, open circuit voltage of 0.9 V and a current density of 14.9  $\text{mA}/\text{cm}^2$  under one-sun illumination.

## 1. INTRODUCTION

Silicon solar cells that possess all back contacts have been extensively explored [1,2]. This type of cell has the advantage of all metallization residing on the back of the cell, giving the opportunity to independently optimize the front and back of the cell for optical and electrical performance, respectively [3]. Back-contacted solar cells are ideal for concentration applications and researchers have been able to create 27.5% efficient silicon cells under 100 suns [4]. This technology has been developed for silicon, an indirect bandgap semiconductor, which requires a thick layer of material to absorb the solar spectrum.

GaAs, on the other hand, is a direct bandgap material capable of absorbing 99% of the solar spectrum (above 1.42 eV) in the first few micrometers. GaAs is used extensively as one of the primary junctions for multi-junction photovoltaic (PV) cells for space applications and concentrator modules. Despite the advantages outlined above, GaAs cells with all back contacts have not been widely explored or reported. Some of the impediments to achieving a GaAs back-contacted solar cell are the complex layered structure and the difficulties involved in doping GaAs from external sources.

Microsystems-enabled photovoltaics is an emerging area that allows the application of reliable and precise manufacturing processes used in the microsystem arena to develop high quality, ultrathin, small form factor PV cells [5]. At these small dimensions, the material usage is drastically reduced and carrier collection is improved [6].

Other efforts to reduce the size of the cells have been undertaken by groups in industry [7,8] and academia [9,10], aiming mainly to interface the small scale cells with mini-concentrators. Using our approach, the cells can be used with micro-concentrators in even smaller packages that would be virtually flat.

In this paper, we present the fabrication, characterization, and testing of a newly developed, all back-contacted GaAs single junction solar cell.

## 2. CELL FABRICATION

The initial semiconductor stack was grown by metal organic vapor phase epitaxy at the National Renewable Energy Laboratory (NREL). This structure is presented in Figure 1. Absorption



**Figure 1. Initial GaAs layer stack for the solar cell provided by NREL.**

The design of the photolithographic masks that define the shape, size, and metallization of the wafer was done using AutoCAD 2008. Hexagonal solar cells were designed in 4 different sizes: 2 mm, 1 mm, 500  $\mu\text{m}$ , and 250  $\mu\text{m}$ . Each size had two design variations with different densities of etch release holes. The release holes are perforations that go all the way from the front of the wafer to the release layer so the chemistry can access the release layer. A section of the AutoCAD design for 500  $\mu\text{m}$  cells is shown in Figure 2. Each colored outline in the figure represents a process performed to the stack to achieve a back-contacted solar cell.

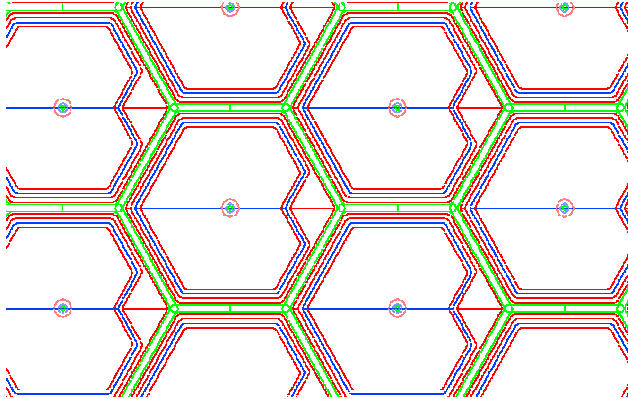


**Figure 2** AutoCAD designs of photolithographic masks for processing of the cell.

The initial GaAs wafer was patterned using standard photolithography. In order to remove the top 4 layers, a series of wet etches followed, landing on the 1  $\mu\text{m}$  GaInP layer. This step defined the active device layer. Figure 3 shows a schematic of the steps required to define, metalize, and release the cells.

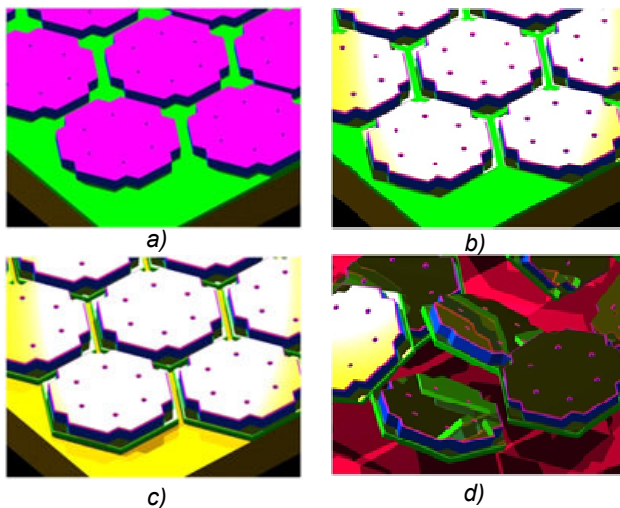


**Figure 3.** Sequence for solar cell release (1 mm design shown). a) the device area of the cells is defined; b) metallization; c) a directional etch to access the release layer; d) submersion of the cells in the etch solution to release the cells.

The top 50 nm GaAs layer was removed by submerging the wafer for 12 seconds in a 1:4:45 solution of  $\text{H}_3\text{PO}_4:\text{H}_2\text{O}_2:\text{H}_2\text{O}$ . The second etch targeted the GaInP layer using a 7:1 solution of  $\text{H}_3\text{PO}_4:\text{HCl}$  in which the wafer was submersed for 14 seconds. Lastly, the same chemistry used to remove the top 50 nm GaAs layer was employed to remove the 1.7  $\mu\text{m}$  GaAs p and n layers submerging the wafer for 462 seconds. The advantage of using this chemistry is its selectivity, as it only etches the GaAs leaving the GaInP intact.

After the wet etches and a cleaning step, the second photolithography mask was used to define the metal pads. After the photoresist (PR) pattern was formed, a metal layer was deposited and PR was removed to lift-off unwanted metal. The metal layer is composed of 10 nm of chromium (to enhance adhesion) followed by 100 nm of gold.

The final photolithographic step defined the size of the cells and the release holes. Photoresist protected the cells, while leaving the boundaries between individual cells uncovered. The wafer went through a reactive ion etch (RIE), removing material to access the AIAs release layer. Figure 4 shows a scanning electron microscope (SEM) image of the cells on the wafer just before release.

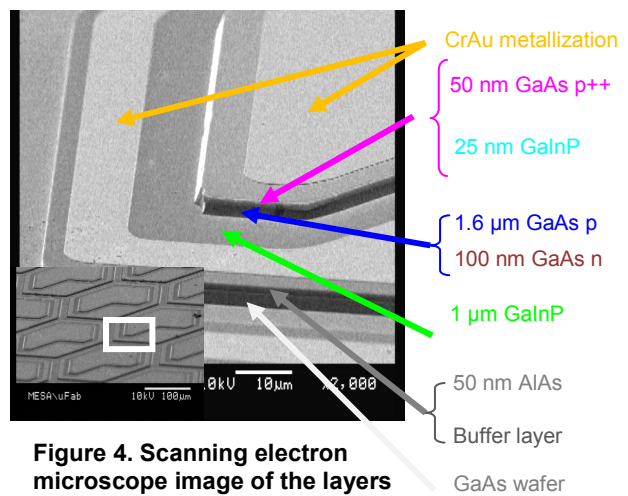


**Figure 4.** Scanning electron microscope image of the layers formed in the processing steps

With the release layer accessible, the wafer was submerged in an HF-based solution to detach the cells from the wafer. The sacrificial layer (AIAs) was selectively etched using a solution composed of 49% HF in water with Tergitol, which is added to prevent the parts from sticking to the wafer once released. Given the small part size, this lift-off process was finished in eight minutes in contrast to the several days required for epitaxial lift-off of a full wafer. As in other lift-off processes, only the device layer is removed which allows the handle wafer to be employed as starting material for further fabrication runs, preserving a substantial amount of expensive material. Figure 5 depicts the cells before, during, and after the release process.

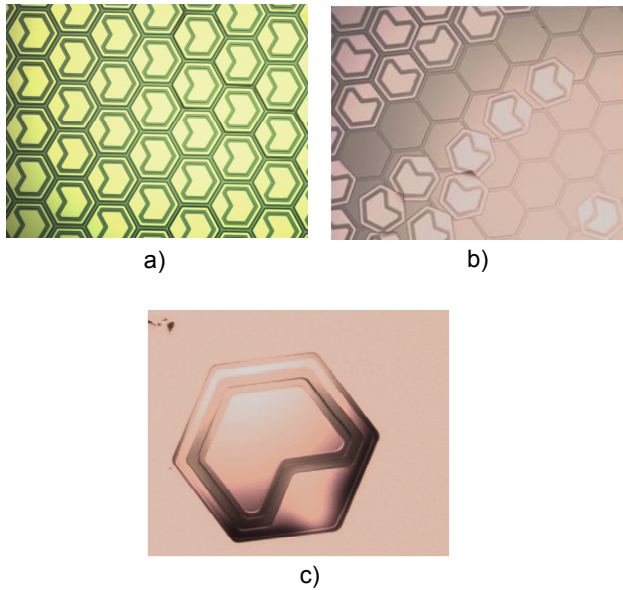


**Figure 5. a) unreleased array of cells. b) cells in the process of being released. c) released cell. The shadows on the released cells indicate curvature of the cells, resulting from residual stress in the layer stack.**

### 3. RESULTS

#### 3.1 Cell releases

Solar cells were released from the handle wafer in a short time (less than 10 minutes) with a yield >90%. However, some bowing in the cells was observed. This curvature was observed in cells with and without metal, indicating that the residual stress resulted from the material layers creating the cell structure. The residual stress from the layers creates two scale-dependent problems. First, as the size of the cell increases, the center to edge height difference increases, making contacting the cells more complicated. Second, the larger cells were also more prone to break when being handled. Another possible effect of the residual stress is that the larger cells (with more release holes) had cracks in between the release holes. This residual stress appears to be due to a minor lattice mismatch between the GaInP and GaAs layers. For electrical testing, we were only able to test cells with sizes up to 1 mm. Larger cells were too curved to be tested effectively and too fragile to connect and assemble. We have a clear path to reduce the warping by changing the thicknesses of the stressed layers.

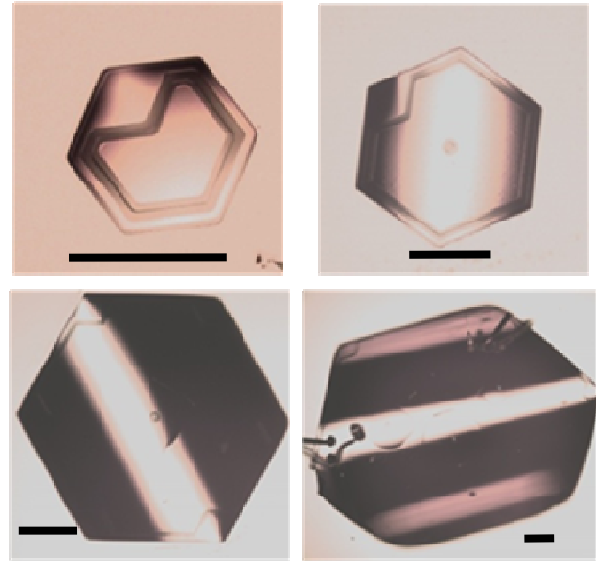


**Figure 6. The four sizes of the cells are shown. From left to right 250  $\mu\text{m}$ , 500  $\mu\text{m}$ , 1 mm and 2 mm. The scale bar is 200  $\mu\text{m}$  for each of the pictures.**

#### 3.2 Contacting procedure

Two methods were used to contact the cells: dispensing small amounts of silver paste on the pads, or contact by using gold wire bonds. In the first approach, the cells were placed on a glass slide with the contacts facing up, and a Mikros™ dispensing pen (Nordson-EFD Corp.) was used to dispense small amounts of silver paste onto the pads of the cell. PDMS polymer was used to isolate the two electrodes from each other. After curing the silver paste, the glass slide with cells was flipped so the front of the cell was facing up.

In the wire bonding method, we created three wire bonds on the wafer before release while the cells were still attached to the wafer. These 3 bonds were used as legs later to have the cell standing on the wire bonds. The wire bonds were connected to testing pads by means of silver paste. Figure 7 shows the details of these two contact methods.

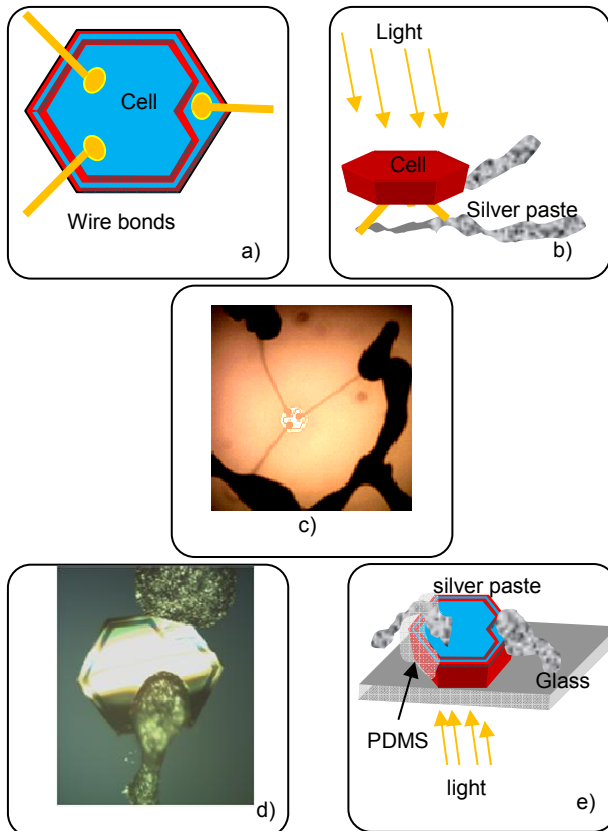


**Figure 7. The two approaches used to contact the cell: Top 3, a), b) and c) figures used silver paste and a standing structure with legs made of gold wire. Bottom 2 figures d) and e): making contact using silver paste and PDMS; illumination is through the glass.**

### 3.2 Electrical characterization

Current versus voltage (IV) curves were obtained using a Spectrolab model XT-10 class A solar simulator with a 1 kW, short arc, xenon lamp. The spectrum was normalized to  $1000 \text{ W/m}^2$  using a silicon reference cell. The temperature during testing was  $25^\circ\text{C}$ . The beam is an 8" X 8" square and the chuck is temperature controlled using thermoelectrics. The solar cell was connected through Kelvin probes to a Keithley model 4200 system with 4210 modules, which was coupled to a custom LabVIEW® VI for data analysis. Figure 8 shows the best results from different sizes and contacting approaches.

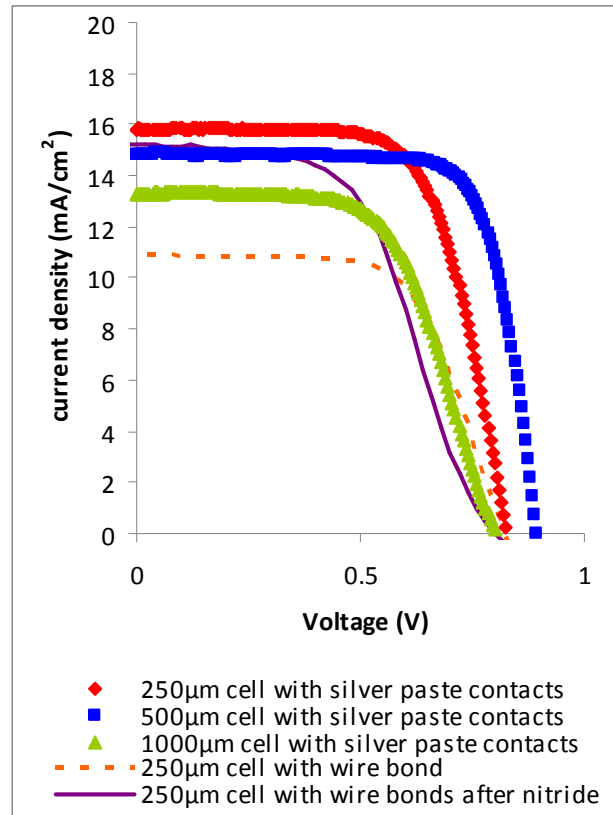


**Figure 8. JV curves of the best cells for different sizes and contacting methods.**

From figure 8, it can be seen that using the silver paste contact method resulted in smaller cells having the largest current collection, and produced the largest series resistance with the lowest  $V_{oc}$  in the 1mm cell. In general, with increasing cell size, we expected to see larger series resistance because of the larger dimensions of the collection sites in the GaInP layer, energy losses due to the increased sheet resistance, and larger  $V_{oc}$  due to diminished recombination on the edges of the cell.

Some of the discrepancies between the predicted and the observed data can be attributed to the bowing of the larger cells.

The data collected from the wire bonded samples shows that the nitride coating (67nm of PECVD nitride used as antireflection coating) increased the collection of carriers but at the same time degraded the contact resistance (seen as higher series resistance), due to the high temperature process used to create the nitride film. The increased current can be attributed to the better absorbance and lower reflection from the cell surface. The difference in current between the 250 µm wire bonded cell and the 250 µm cell contacted with silver paste cell could be attributed to a structural change of the grown layers caused by the high temperature encountered during the wire bonding process.

The base layer in this first trial (p GaAs) is not optically thick and it could be grown thicker to collect more light and generate larger currents.

Our best cell (500  $\mu\text{m}$ ) obtained a  $V_{oc}$  of 895mV, and a current density of 14.9mA/cm<sup>2</sup> with a fill factor of 75%, and conversion efficiency of 10%.

#### 4. CONCLUSIONS

All back-contacted GaAs solar cells were created utilizing techniques and processes from the microsystem arena. The cells ranged in size from 250  $\mu\text{m}$  to 2 mm and the absorbing layer was 1.6  $\mu\text{m}$ . The best cell had a conversion efficiency of 10%.

Silver paste contacts performed better than wire bond contacts. This may be due to the high temperature steps involved in creating the wire bond. Nitride AR coating increased the current but reduced the fill factor in the IV curve.

This approach brings the benefits of back contacts to direct bandgap GaAs solar cells. This allows simplified packaging from having the contacts on the same side. Besides lift-off, small form factor cells also reduce the amount of material used, and thus reduce the cost and weight of the system. When combined with micro-concentrators, further improvements in the overall system cost is also expected due to reduced tracking requirements, unique connectivity, as well as power management approaches enabled by these cells.

#### ACKNOWLEDGEMENTS

Sandia is a multiprogram laboratory operated by Sandia Corporation, a Lockheed Martin Company, for the United States Department of Energy's NNSA under contract DE-AC04-94AL85000. This work was sponsored by the DOE Solar Energy Technology Program Seed Fund.

The authors would like to thank the following MEPV team members for their contributions to this research: Catalina Ahlers, Michael Busse, J. Carapella, Craig Carmignani, Anton Filatov, Jennifer Granata, Robert Grubbs, Rick Kemp, Judith Lavin, Tom Lemp, Tony Lentine, Kathy Meyers, Jeff Nelson, Mark Overberg, David Peters, Carrie Schmidt, Lisa Sena-Henderson, Jerry Simmons, Mike Sinclair, Constantine Stewart, Jason Strauch, Bill Sweatt, Benjamin Thurston, George Wang, and Jonathan Wierer.

#### REFERENCES

---

[1] R.A. Sinton, Y. Kwark, S. Swirhun, and R.M. Swanson, "Silicon Point Contact Concentrator Solar Cells", *IEEE Electron Device Lett.*, **6**, 1985, pp. 405-407  
[2] R.M. Swanson, "Point-Contact Solar Cells: Modeling And Experiment", *Solar Cells* **17**, 1986, pp. 85-118  
[3] J. Dicker, J.O. Schumacher, W. Warta, and S.W. Glunz, "Analysis of One-Sun Monocrystalline Rear-Contacted Silicon Solar Cells with Efficiencies of 22.1%", *J. Appl. Phys.* **91**, 2002, pp. 4335-4343

---

[4] R.A. Sinton, Y. Kwark, S. Swirhun, and R.M. Swanson, "27.5-Percent, Silicon Concentrator Solar Cells", *IEEE Electron Device Lett.*, **7**, 1986, pp. 567-569  
[5] G.N. Nielson, M. Okandan, P. Resnick, J.L. Cruz-Campa, T. Pluym, P. J. Clews, E. Steenbergen, V. P. Gupta, "Microscale C-Si (C)PV Cells For Low-Cost Power", *34<sup>th</sup> IEEE PVSC*, 2009, pp.1816-1821  
[6] G.N. Nielson; M. Okandan; P. Resnick; J.L. Cruz-Campa; P.J. Clews; M. Wanlass; W.C. Sweatt; E. Steenbergen; V.P. Gupta, "Microscale PV Cells For Concentrated PV Applications", *24<sup>th</sup> EU PVSEC*, 2009, pp.170-173  
[7] W.P. Mulligan, A. Terao, D.D. Smith, P.J. Verlinden, and R.M. Swanson, "Development of Chip-Size Silicon Solar Cells", *28<sup>th</sup> PVSC*, 2000, pp. 158-163  
[8] K.J. Weber, A.W. Blakers, M.J. Stocks, J.H. Babaei, V.A. Everett, A.J. Neuendorf, and P.J. Verlinden, "A Novel Low-Cost, High-Efficiency Micromachined Silicon Solar Cell" *IEEE Electron Device Lett.* **25**, 2004, pp. 37-39  
[9] X. Guoa, H. Li, B.Y. Ahn, E.B. Duoss, K.J. Hsia, J.A. Lewis, and R.G. Nuzzo, "Two- and Three-Dimensional Folding of Thin Film Single-Crystalline Silicon for Photovoltaic Power Applications", *PNAS* **106**, 2009, pp. 20149-20154  
[10] B. Tian, X. Zheng, T. J. Kempa, Y. Fang, N. Yu, G. Yu, J. Huang & C. M. Lieber, "Coaxial Silicon Nanowires as Solar Cells and Nanoelectronic Power Sources", *Nature* **449**, 2007, pp. 885-889